HHS Public Access

Author manuscript

J Immunol. Author manuscript; available in PMC 2016 August 01.

Published in final edited form as:

J Immunol. 2015 August 1; 195(3): 1044–1053. doi:10.4049/jimmunol.1402894.

Bacterial membrane vesicles mediate the release of *Mycobacterium tuberculosis* lipoglycans and lipoproteins from infected macrophages

Jaffre J. Athman[*], **Ying Wang**[*], **David J. McDonald**[†,§], **W. Henry Boom**[‡,§], **Clifford V. Harding**[*,§], and **Pamela A. Wearsch**[*,§]

[*]Department of Pathology, Case Western Reserve University/University Hospitals Case Medical Center, Cleveland, OH

[†]Department of Molecular Biology and Microbiology, Case Western Reserve University/University Hospitals Case Medical Center, Cleveland, OH

[‡]Division of Infectious Diseases, Case Western Reserve University/University Hospitals Case Medical Center, Cleveland, OH

[§]Center for AIDS Research, Case Western Reserve University/University Hospitals Case Medical Center, Cleveland, OH

Abstract

Mycobacterium tuberculosis (Mtb) is an intracellular pathogen that infects lung macrophages and releases microbial factors that regulate host defense. Mtb lipoproteins and lipoglycans block phagosome maturation, inhibit MHC-II antigen presentation, and modulate TLR2-dependent cytokine production, but the mechanisms for their release during infection are poorly defined. Furthermore, these molecules are thought to be incorporated into host membranes and released from infected macrophages within exosomes, 40-150 nm extracellular vesicles that derive from multivesicular endosomes. However, our studies revealed that extracellular vesicles released from Mtb-infected macrophages include two distinct, largely non-overlapping populations, one containing host cell markers of exosomes (CD9, CD63) and the other containing Mtb molecules (lipoglycans, lipoproteins). These vesicle populations are similar in size, but have distinct densities as determined by separation on sucrose gradients. Release of Mtb lipoglycans and lipoproteins from infected macrophages was dependent on bacterial viability, implicating active bacterial mechanisms in their genesis. Consistent with recent reports of extracellular vesicle production by bacteria (including Mtb), we propose that bacterial membrane vesicles are secreted by Mtb within infected macrophages and subsequently released into the extracellular environment. Extracellular vesicles released from Mtb-infected cells activate TLR2 and induce cytokine responses by uninfected macrophages. We demonstrate that these activities derive from the bacterial membrane vesicles rather than exosomes. Our findings suggest that bacterial membrane vesicles are the primary means by which Mtb exports lipoglycans and lipoproteins to impair effector functions

Corresponding Author: Pamela A. Wearsch, Dept. of Pathology, Case Western Reserve University, 2103 Cornell Rd, Cleveland, OH 44106 USA, Tel: 216-368-5059, Fax: 216-368-0494, paw28@case.edu.

within infected macrophages and circulate bacterial components beyond the site of infection to regulate immune responses by uninfected cells.

Keywords

Extracellular vesicles; bacterial membrane vesicles; exosomes; *Mycobacterium tuberculosis*; macrophage

Introduction

Mycobacterium tuberculosis (Mtb) is an intracellular pathogen that primarily infects macrophages in the lung and establishes latent infection. To create a niche within the phagosome of infected cells, Mtb secretes molecules that modulate the host immune response. Many of these molecules are derived from the Mtb cell wall and are secreted during the course of infection. These factors include the lipoglycan LAM (lipoarabinomannan) which inhibits phagosome maturation (1) and lipoproteins which are potent agonists of TLR2 (2). Although activation of TLRs typically promotes immunity, prolonged TLR2 signaling by Mtb inhibits MHC-II antigen presentation to CD4+ T cells (2-6) and may induce other immune suppressive mechanisms, e.g. via IL-10 (7-9).

After their shedding from Mtb bacilli, cell wall components such as lipoglycans and lipoproteins are disseminated throughout the endocytic network of infected macrophages and may act on host targets (10). In addition, infection of macrophages with mycobacteria leads to the release of extracellular vesicles (EVs) that contain numerous mycobacterial lipoglycans, lipoproteins, and antigens (11-15). EVs are small vesicles (< 1 μm) released by all cell types studied to date that function in intercellular communication or transfer (16). EVs from macrophages infected with Mtb, *M. bovis* BCG, or *M. avium* activate proinflammatory responses, drive DC maturation, and regulate MHC-II antigen presentation, consistent with the EV-associated bacterial cargo (11, 12, 17-20). It has been proposed that the vesicles mediating these immunomodulatory functions are exosomes, 40-150 nm EVs that are constitutively secreted by mammalian cells via fusion of multivesicular endosomes (MVEs) with the plasma membrane (11, 12) (15, 16, 21, 22). This model was first suggested by electron microscopy images of vesicle-mediated exocytosis of bacterial components from *M. bovis* BCG-infected macrophages (14, 15) and has been the foundation for subsequent studies (11-13, 15, 18-20). A major premise of this model is that Mtb lipoglycans and lipoproteins associate with host membranes and traffic into MVEs (11, 12, 15). However, the mechanisms for the secretion of membrane-associated Mtb components and trafficking into EVs have not been defined.

Since EVs released by Mtb-infected macrophages may have a profound influence on host responses to Mtb *in vivo*, we sought to better understand the nature and origin of EVs that are released by Mtb-infected macrophages. Using a combination of biochemical and imaging analyses, we observed that the EVs produced during Mtb infection are heterogeneous. Contrary to the model that exosomes mediate the export of Mtb molecules from infected cells, our characterization of EVs released by Mtb-infected cells demonstrated the existence of a vesicle subpopulation that contained Mtb molecules and were distinct

from EVs that expressed markers of exosomes. Concurrent with these studies was a report that Mtb produces EVs in axenic culture that are enriched for Mtb lipoglycans and lipoproteins (23). Our further characterization of EV subpopulations supported the hypothesis that Mtb molecules released by infected macrophages are contained in bacterial membrane vesicles (BMVs) derived from intracellular Mtb as opposed to host membrane-derived exosomes. This conclusion is consistent with our observation that the release of EVs containing Mtb molecules was dependent on Mtb viability, suggesting that active bacterial secretion processes are required to produce BMVs that are subsequently released from macrophages. Finally, we separated exosomes from BMVs and tested each fraction for biological activities previously described for the EVs released by Mtb-infected cells. BMVs, but not exosomes, induced TLR2 signaling as well as cytokine production by uninfected macrophages, consistent with the enrichment of Mtb lipoproteins in the BMV fraction. Taken together, our results support the hypothesis that Mtb releases BMVs within infected macrophages that are subsequently released into the extracellular environment. Furthermore, these data suggest an important role for Mtb BMVs in the regulation of infected and uninfected cells that likely contributes to the pathogenesis of Mtb infection.

Materials and Methods

Reagents and antibodies

BSA, chemicals, detergents, and protease-free sucrose were purchased from Sigma-Aldrich (St. Louis, MO). Normal donkey serum and gold-conjugated secondary antibodies were obtained from Jackson Immunoresearch (West Grove, PA). Electron microscopy grade formaldehyde was purchased from Thermo Fisher (Waltham, MA) and used for all imaging experiments. Antibodies employed for Western blotting included rabbit anti-Mtb polyclonal Ab (Genway Biotech, San Diego, CA), anti-LpqH clone IT-19 (hybridoma from BEI Resources, Manassas, VA), anti-mouse CD9 clone EM-04 (Pierce, Rockford, IL), anti-mouse CD63 clone NVG-2 (Biolegend, San Diego, CA), and anti-GAPDH (Pierce). Antibodies employed for imaging experiments included rabbit anti-Mtb polyclonal Ab (Genway Biotech), anti-MHC-II clone Y3P (anti-IA^b; hybridoma from ATCC, Manassas, VA), anti-mouse CD63 clone NVG-2 (Biolegend), and anti-mouse CD9 clone MZ3 (unconjugated and biotinylated, Biolegend). IT-19 and Y3P mAb were purified from hybridoma culture supernatants using protein G affinity chromatography. The polyclonal anti-Mtb Ab detects LAM and LM, although its specificity is not limited to these lipoglycans. Rabbit IgG and rat IgG2a isotype controls were purchased from Thermo Fisher and Biolegend, respectively. Fluorochrome-conjugated secondary detection reagents included DyLight 488 anti-rabbit IgG (Biolegend), Alexa Fluor 555 anti-rat IgG (Molecular Probes, Eugene, OR), and streptavidin-Alexa Fluor 647 (Molecular Probes).

Bacterial culture

Mtb strain H37Ra was obtained from American Type Culture Collection (Manassas, VA). Bacteria were cultured at 37°C in Middlebrook 7H9 broth (Difco, Detroit, MI) supplemented with 10% ADC (BD), 0.05% Tween 80, and 0.2% glycerol. Bacteria were grown to mid-log phase (OD_{600} = 0.5 to 0.6) and frozen in 25% glycerol for infection stocks. The titer of the infection stocks was determined by serial dilution on Middlebrook

7H11 agar plates after declumping with seven passages through a 25-gauge needle and centrifugation at 100 × *g* for 5 min.

Mammalian cell culture

All animal studies were approved by the Institutional Animal Care and Use Committee of Case Western Reserve University. C57BL/6J mice (8-12 week old female) were obtained from Jackson Laboratory (Bar Harbor, ME) and housed under specific pathogen-free conditions. All references to macrophages indicate the use of bone marrow-derived macrophages with the exception of purification of Mtb bacilli from infected RAW264.7 cells (described below). Macrophages were cultured from suspensions of bone marrow cells as described previously (24). Briefly, bone marrow was flushed from femurs and tibias, and cell suspensions were homogenized and filtered through a 70-μm screen. Bone marrow cells were cultured in DMEM (HyClone, Logan, UT) supplemented with 10% heat-inactivated fetal bovine serum (Gibco, Carlsbad, CA), 50 μM 2-mercaptoethanol (Bio-Rad, Hercules, CA), 1 mM sodium pyruvate (HyClone), 10 mM HEPES (HyClone), 100 units/ml penicillin, and 100 μg/ml streptomycin (HyClone) with 25% LADMAC cell conditioned medium as a source of M-CSF. Unless otherwise indicated, all incubations with macrophages were at 37°C in a humidified, 5% CO_2 atmosphere. The medium was changed on days 5 and 7 of culture, and macrophages were used on day 8. HEK293/hTLR2-CD14 cells (Invivogen, San Diego, CA) were cultured in DMEM supplemented with 10% FCS, 100 μg/ml Normocin (Invivogen), 10 μg/ml Blasticidin (Invivogen), and 50 μg/ml HygroGold (Invivogen). HEK293.pcDNA3 vector control cells were cultured in DMEM supplemented with 10% FCS and 500 μg/ml Geneticin.

Infection of macrophages and EV purification

Macrophages were plated on 150 mm dishes and allowed to recover for 1 d prior to infection. Cells were washed and then infected with H37Ra at a multiplicity of infection (MOI) of 0-6 in antibiotic-free, supplemented DMEM. Where indicated, bacteria were killed prior to infection by treatment at 80°C for 30 min or by exposure to 60,000 rad using a ^{137}Cs source (25). After 4 h macrophages were washed four times with 10 mL of PBS to remove extracellular bacteria. (Complete removal of extracellular bacteria was supported by the observation that no detectable yield of EVs was recovered from macrophage-free control plates that were treated with bacteria for 4 h and washed, data not shown). The medium was replaced with antibiotic-free supplemented DMEM that was centrifuged prior to use at 100,000 × *g* for 18 h to remove exosomes that are present in FBS (vesicle production medium), and the cells were cultured for an additional 20 h (24 h total infection time). The viability of Mtb-infected macrophages was > 90% at 24 h post-infection. EVs released by uninfected or Mtb-infected macrophages were purified by differential ultracentrifugation using established protocols (26). To remove cells and larger particulates, the culture medium was centrifuged at 4°C sequentially at 500 × *g* for 15 min, 2000 × *g* for 15 min, and 10,000 × *g* for 30 min (at each step harvesting the supernatant). The clarified supernatant was then centrifuged at 100,000 × *g* for 70 min using the Beckman SW28 rotor to pellet EVs. The vesicle pellet was washed in PBS and recovered by centrifugation for 70 min at 100,000 × *g* using the Beckman TLA100.3 rotor. The final EV pellet was suspended in PBS to give a concentration of vesicles produced from 10^6 cell equivalents per μl; this preparation

constitutes EVs purified by differential centrifugation. Purified EVs were analyzed immediately or frozen in aliquots at −80°C. Of note, a final centrifugation step at 100,000 × *g* for 1 h has been employed as a standard approach to isolate exosomes (26), EVs released by Mtb-infected cells (11, 12, 14), and BMVs from Mtb axenic cultures (23). Thus, the EV purification methods employed here and in past studies (11, 12, 14) will recover both exosomes and Mtb BMVs with high efficiency.

Where indicated, EV subpopulations were separated by sucrose density gradient centrifugation. EVs were first purified by differential centrifugation as described above from 1.5×10^8 macrophages infected with Mtb at an MOI of 5. The 100,000 × *g* pellet was resuspended in 200 μl of PBS, overlaid on a 11.5 ml continuous sucrose gradient (0.2-1.8 M sucrose with 10 mM HEPES, pH 7.2), and centrifuged for 19 h at 110,000 × *g*. Fractions of 1 ml were collected from the top of the gradient, weighed to determine their density, and concentrated by TCA precipitation. The content of each fraction was analyzed by 12% SDS-PAGE and Western blotting for exosome markers or Mtb molecules.

qNano analysis of EVs

The qNano instrument (Izon, Oxford, UK) allows the determination of vesicle size by tunable resistive pulse sensing. This technique involves passing individual particles in suspension through a membrane with pores of a defined size while maintaining a constant voltage applied across the membrane. By measuring changes in the current as particles pass through the pore, the instrument calculates the diameter of particles (modeled as spherical). Purified EVs were diluted in 2X PBS (200 mM NaCl in 13 mM sodium phosphate) and analyzed with the qNano using NP150 nanopore membranes in comparison to 100 nm calibration particles run under identical conditions. Data were analyzed using Izon Control Suite software version 2.2.

Western blotting

Samples were analyzed by 12% SDS-PAGE (under non-reducing conditions for CD9 and CD63 blots and reducing conditions for all others) and transferred to Immobilon PVDF membranes (Millipore). Membranes were incubated in blocking buffer (5% milk in PBS with 0.1% Tween), followed by incubation with primary antibodies overnight at 4°C in blocking buffer. Membranes were washed and then incubated with HRP-conjugated secondary antibodies (Jackson Immunoresearch, West Grove, PA) for 1 h at room temperature. Membranes were washed three times in PBS with 0.1% Tween and detection was performed with ECL Western blotting substrate (Pierce).

Whole mount electron microscopy

For the production of EVs for electron microscopy analysis, macrophages were treated with 2 ng/ml IFN-γ (to induce MHC-II expression) for 16 h prior to infection. Cells were infected with Mtb at MOI of 3 and the EVs were purified as described above. The washed 100,000 × *g* pellet was fixed in 2% electron microscopy grade formaldehyde overnight at 4°C and processed for whole mount electron microscopy as described (26). The following steps were performed at room temperature unless otherwise noted. EVs were adsorbed by inversion of formvar-carbon grids onto 10-15 μl drops for 20 min. Grids were then floated sequentially

on droplets of PBS (twice for 3 min), on droplets of PBS with 1% BSA (10 min), primary Ab (40 min), 1% BSA (six times for 3 min), secondary Ab (40 min) and 1% BSA (three times for 3 min), and on droplets of PBS (three times for 3 min). Primary Abs were used at the following concentrations: 10 μg/ml anti-CD9, 20 μg/ml anti-MHC-II clone Y3P, and 5 μg/ml Genway anti-Mtb. Parallel EV samples were stained with the same concentration of the appropriate isotype-matched control antibody to confirm the specificity of labeling. Colloidal gold-conjugated secondary Abs were 5 nm anti-rabbit IgG, 10 nm anti-mouse IgG, and 18 nm anti-rat IgG. The grids were then floated on droplets of 1% glutaraldehyde (2 min), 10 mM glycine (5 min), distilled water (eight times for 2 min), 4% uranyl acetate with 0.075 M oxalic acid (5 min), and a mixture of 1 part 4% uranyl acetate and 9 parts 2% methyl cellulose (10 min on ice). Images were obtained using a JEOL 1200 EX transmission electron microscope.

Immunofluorescence microscopy

The following steps were performed at room temperature. Frozen stocks of purified EVs were thawed and fixed in a final concentration of 2% electron microscopy grade formaldehyde, immediately spotted onto #1 coverslips (Thermo Fisher) and allowed to adhere for 20 min in a humidified chamber. Coverslips were then incubated for 20 min with 150 μl of 2% electron microscopy grade formaldehyde, washed three times with 150 μl PBS, and blocked for 30 min with 10% normal donkey serum in PBS. Two sequential labeling steps were performed. First, coverslips were incubated for 30 min with 5 μg/ml anti-CD63 or anti-CD9, washed three times with 150 μl PBS, incubated for 30 min with 5 μg/ml Alexa Fluor 555 anti-rat IgG, washed three times with PBS and blocked for 30 min with 5 μg/ml rat IgG. For the second labeling step, coverslips were incubated for 30 min with 5 μg/ml biotinylated anti-CD9 or 20 μg/ml anti-Mtb, washed three times with 150 μl PBS wash, incubated for 30 min with 40 μg/ml streptavidin-Alexa Fluor 647 or 5 μg/ml DyLight 488 anti-rabbit, and washed three times with PBS. Coverslips were mounted onto microscope slides using ProLong Gold with DAPI (Molecular Probes). Slides were cured overnight and imaged using a Deltavision RT epifluorescence microscope with a 100X 1.4 NA objective (Applied Precision, Issaquah, WA). A minimum of 15 images were captured per sample and deconvolved using the Softworx software package (Applied Precision). The average maximum signal intensity for 15 isotype control images was employed as the level of background staining and was set as the lower threshold cutoff for all images. Colocalization was determined as the number of particles fluorescent in both image channels by the Spatial Pearson's Coefficient Algorithm available in the JACoP plugin for ImageJ (NIH). The number of dual-stained and single-stained points was quantified using the ImageJ Analyze Particles function.

Isolation of Mtb bacilli from infected macrophages

Adherent RAW 264.7 cells (ATCC; 3×10^6 cells per well in 6-well plates) were incubated with live or heat-killed Mtb at an MOI of 20 in supplemented DMEM media without antibiotics for 20 min. During the infection step, the plates were centrifuged at $1,000 \times g$ for 10 min followed by an additional 10 min incubation at 37° C. The macrophages were then washed extensively to remove extracellular bacteria and incubated for an additional 40 min at 37°C. The following steps were performed at 4°C. The cells were washed with PBS,

harvested by scraping, washed with PBS, resuspended in homogenization buffer (0.25 M sucrose with 10 mM HEPES, pH 7.2) and disrupted using a Dounce homogenizer until ~ 80% cell lysis was observed by trypan blue staining. The cell lysate was centrifuged at 100 × *g* for 3 min to remove intact cells and nuclei. The supernatant was centrifuged at 550 × *g* for 15 min. The pellet, containing Mtb bacilli and mitochondria, was resuspended in 1 ml of homogenization buffer, overlaid on 9 ml of 40% Percoll (Sigma), and centrifuged at 36,000 × *g* for 1 h. The bacterial layer was collected, diluted 3-fold with PBS and centrifuged at 6000 × *g*. The resulting pellet was fixed in 2% formaldehyde, and processed for electron microscopy.

Purification of vesicle subsets and functional analysis

EVs released from 2.5×10^8 Mtb-infected macrophages were prepared and fractionated on sucrose density gradients as described above. Fractions (1 mL each) were collected, screened, and pooled into three sets: control (fractions #2-4, no EVs), exosomes (fractions #5-7 containing CD9 and CD63, but little Mtb content), and BMVs (fractions #8-10 containing Mtb lipoglycans and lipoproteins, but little exosome content). The pooled fractions were concentrated using Amicon Ultra centrifugal filters with 10 kDa m.w. cut off (Millipore) and exchanged into a final volume of 150 μl DMEM. To determine the TLR2 stimulatory capacity of the EV subsets, HEK293/hTLR2-CD14 cells or HEK293.pcDNA3 control cells (5×10^4 cells per well) were treated in duplicate with 17.5 μL of each fraction in a final volume of 100 μL. The supernatants were harvested at 24 h and IL-8 production was quantitated by ELISA using the human IL-8 DuoSet (R&D Systems, Minneapolis, MN). To determine the effect of each EV subset on cytokine production by uninfected macrophages, murine bone marrow-derived macrophages (10^5 cells per well) were treated in duplicate with 17.5 μL of each fraction in a final volume of 100 μL. The supernatants were harvested at 24 h and TNF-α production was quantitated by ELISA using the murine TNF-α DuoSet (R&D Systems).

Results

Mtb-infected macrophages release EVs that contain exosome markers and Mtb molecules

The goal of these studies was to investigate the trafficking of Mtb cell wall components into EVs that are released by Mtb-infected macrophages. We employed an experimental approach similar to prior studies (11-14, 18, 19) for the purification of EVs that are produced during Mtb infection. Macrophages were infected *in vitro* with Mtb strain H37Ra for 4 h, washed extensively to remove extracellular bacteria, and cultured for an additional 20 h to allow EVs to accumulate in the culture medium. At 24 h post-infection the conditioned medium was harvested and EVs were purified by differential ultracentrifugation. Analysis by tunable resistive pulse sensing using the IZON qNano system indicated the presence of EVs with sizes predominantly in the range of 85-150 nm with a mode (peak) diameter of 95-105 nm (Fig. 1A). The size distribution and mode diameter of EVs released by uninfected and Mtb-infected cells were similar (Fig. 1A). These results are consistent with the size of exosomes (40-150 nm), but other types of EVs have sizes in this range. We next analyzed the biochemical composition of EVs released by Mtb-infected and uninfected macrophages by Western blotting. CD9, CD63, Alix and LAMP1,

which are markers that are highly expressed in exosomes, were detected in EVs (Fig. 1B and data not shown). Infection of macrophages with Mtb caused a decrease in release of some exosome markers in the EV fraction (e.g., CD63 in Fig. 1B), but the magnitude of this change was not consistent among exosome markers and showed some experimental variation, so its significance is unclear. EVs from Mtb-infected macrophages contained Mtb components, including lipoglycans (LAM and LM) and lipoproteins (LpqH and LprG) (Fig. 1C and data not shown). We conclude that EVs released by Mtb-infected macrophages contain both host exosome markers and Mtb molecules.

Electron and fluorescence microscopy reveal distinct vesicle populations that contain host- or Mtb-derived molecules

The studies in Fig. 1 and in previous reports demonstrate that the EVs released from infected cells have properties that are consistent with exosomes (based on size and isolation methods). However, these properties are not specific to exosomes and may be shared by other EVs. Moreover, the approaches used in these studies did not distinguish whether the EVs are homogeneous or contain subpopulations of EVs with potential differences in composition and function. To further characterize the EVs that disseminate Mtb components from infected cells, we purified EVs from Mtb-infected macrophages and performed whole mount electron microscopy with immunogold labeling. In this procedure, EVs are mounted on a carbon grid and contrast-stained, yielding a 3-dimensional cup-like appearance (26). The morphology and sizes of EVs released by Mtb-infected cells (Fig. 2A) were consistent with those described for exosomes in the literature. Single immunogold labeling revealed that the EVs contained MHC-II molecules, a component of exosomes released by macrophages (17, 27); they also contained Mtb molecules, as demonstrated by immunogold labeling with a polyclonal anti-Mtb Ab that recognizes Mtb lipoglycans (Fig. 2B, C). However, when dual immunogold labeling was performed, virtually no EVs were observed that contained both MHC-II and Mtb molecules (Fig. 2D). This finding was repeated when EVs purified from Mtb-infected cells were triple-labeled using antibodies against Mtb, MHC-II and CD9 (an exosome marker). Colocalization of CD9 and MHC-II in vesicles was frequently observed, but Mtb components were not present in $CD9^+$, $MHC\text{-}II^+$, or $CD9^+$/$MHC\text{-}II^+$ vesicles (Fig. 2E). Instead, labeling for Mtb components was observed in a separate population of EVs. These data indicate that the EVs released by Mtb-infected macrophages are heterogeneous and suggest that Mtb molecules are present in a vesicle population that is distinct from exosomes.

To assess EV heterogeneity using a quantitative approach, we developed a method for the analysis of EVs using immunofluorescence microscopy. EVs produced by Mtb-infected macrophages were purified, fixed to glass coverslips, and stained for host or Mtb molecules. The presence of two components within a vesicle was determined by colocalization analysis (see Materials and Methods). Fig. 3 shows representative images of EVs using this technique. A high degree of colocalization was observed for EVs stained for CD9 and CD63, two commonly employed exosome markers (Fig. 3A). In contrast, Mtb molecules were largely excluded from the $CD63^+$ or $CD9^+$ exosome populations (Fig. 3B). Quantification of 15 images per sample in two independent experiments indicated that only $3.5 \pm 0.5\%$ of Mtb^+ EVs contained CD9, and $13 \pm 4.1\%$ of Mtb^+ EVs contained CD63,

whereas 51 ± 1.5% of $CD9^+$ EVs contained CD63, and 45 ± 4.6% of $CD63^+$ EVs contained CD9 (Fig. 3C). Over the course of many imaging experiments, the proportion of EVs containing Mtb molecules was approximately 10-20% of all labeled vesicles (Fig. 3; data not shown). These data confirm the findings from electron microscopy studies (Fig. 2) and establish that the majority of EVs that contain Mtb molecules are distinct from host-derived exosomes.

Subpopulations of EVs released by Mtb-infected cells can be separated using sucrose density gradients

To examine the apparent heterogeneity of EVs using an independent experimental approach, the EVs derived from Mtb-infected macrophages were analyzed using sucrose density gradients. EVs were purified from Mtb-infected cells by differential centrifugation, overlaid on a 0.2-1.8 M sucrose density gradient, and centrifuged for 19 h at 110,000 × *g*. Gradient fractions were collected and analyzed by Western blotting for Mtb molecules or exosome marker proteins (Fig. 4). Both CD9 and CD63 were present in EVs with a peak in fraction #6 (density of 1.11 g/ml); the labeling properties and density of these EVs are consistent with exosomes (27, 28). In contrast, the Mtb lipoglycans LAM and LM were present in EVs with a peak in fraction #9 (density of 1.17 g/ml); this fraction did not contain CD9 or CD63. These results confirm the presence of two distinct vesicle populations of EVs released by Mtb-infected macrophages and suggest that the vesicles in fraction #9 are not exosomes. The overlap of host and Mtb molecules in fractions #7-8 is likely due to the incomplete separation of two distinct vesicle populations on the gradient, but a small degree of Mtb lipoglycan incorporation into exosomes is also possible. We conclude that the vast majority of Mtb components were present in a subset of EVs that could be physically separated from exosomes by sucrose density centrifugation, consistent with a unique cellular origin.

Evidence for active production of bacterial membrane vesicles by Mtb during infection of macrophages

We next sought to identify the origin of EVs that contain Mtb lipoglycans and lipoproteins. Since the EVs containing Mtb molecules were distinct from exosomes and were not consistent with the properties of other types of mammalian EVs, such as microvesicles, we considered the possibility that they were produced by the bacteria. It has been recently established that 20-300 nm bacterial membrane vesicles (BMVs) are produced by a wide range of bacterial species, including Mtb (23, 29-33). Since the production of Mtb BMVs is an active secretion process by live bacteria (23), we investigated the requirement for bacterial viability for incorporation of Mtb molecules into EVs. To this end, Mtb stocks were killed by heat treatment or irradiation using established protocols (25). Macrophages were incubated for 4 h with live Mtb, heat-killed Mtb or irradiated Mtb, washed and incubated for 20 h. Of note, our prior studies revealed no significant differences in macrophage uptake of live Mtb vs. Mtb killed by these methods (25). EVs were isolated from the culture medium by differential ultracentrifugation and analyzed by Western blotting. The level of LAM and LM released in EVs was substantially reduced in macrophages exposed to heat-killed or irradiated Mtb relative to macrophages exposed to viable Mtb (Fig. 5A). This was particularly true for heat-killed Mtb, which produced essentially no detectable release of LAM and LM in EVs from the macrophages. Although

not replication-competent, irradiated Mtb maintains short-term molecular functions, likely explaining the persistence of low levels of BMV production and release from macrophages. These data support a mechanism for the trafficking of Mtb lipoglycans into EVs that requires active bacterial processes. Furthermore, these findings are consistent with the conclusion that Mtb BMVs are released by Mtb-infected cells into the extracellular environment.

Our emerging model postulates that Mtb BMVs are produced within infected cells and are subsequently exocytosed by Mtb-infected macrophages. To further address this model, we sought evidence for the intracellular production of BMVs by Mtb in macrophages. Since BMV production is difficult to observe in thin sections of Mtb-infected cells, we isolated Mtb bacilli from infected cells prior to processing for electron microscopy. RAW264.7 cells were infected for 1 h and then disrupted by Dounce homogenization to release intracellular bacteria. Mtb bacilli were purified from the macrophage extracts and processed for transmission electron microscopy. Structures resembling budding vesicles were associated with the surface of Mtb bacilli (Fig. 5B). No such structures were observed with heat-killed bacteria (Fig. 5C). The vesicle-like structures observed on viable intracellular bacteria were approximately 50 nm in diameter, consistent with the reported size of BMVs produced by Mtb axenic cultures (23). Because of significant technical differences, the vesicle diameters measured by qNano (Fig. 1A), whole mount EM (Fig. 2), and TEM (Fig. 5A and (26)) will show some degree of variation. These observations support the conclusion that BMVs are produced by viable intracellular Mtb within infected macrophages. Collectively, our findings support a model in which most Mtb molecules are exported from Mtb-infected macrophages within BMVs as opposed to host membrane-derived exosomes.

The proinflammatory activity of EVs derives from BMVs released by Mtb-infected cells

Since the heterogeneity of EVs released from Mtb-infected cells was previously unknown, we sought to determine whether the exosome subset, the BMV subset, or both subsets contributed to the biological activities of EVs observed in prior work. To this end, we employed sucrose density gradients to fractionate the EVs released from Mtb-infected macrophages and pooled the respective exosome and BMV-containing fractions for use in functional assays. Fractions #5-7 contained CD9 and CD63, the markers of exosomes. In addition to Mtb LAM, fractions #8-10 contained TLR2 agonists such as the lipoprotein LpqH and the lipoglycan LM. Sucrose gradient fractions #2-4 were pooled as a control. Each pool from the sucrose gradient was concentrated and then analyzed by Western blotting to confirm the recovery of vesicles (Fig. 6A).

Functional studies of EVs bearing Mtb components have largely focused on TLR activation and the production of cytokines by uninfected macrophages (11, 12, 19, 23, 32). Accordingly, we tested the ability of fractions #2-4 (control), #5-7 (exosomes), and #8-10 (BMVs) to activate TLR2 using reporter cell lines. HEK cells transfected with control vector or hTLR2-CD14 were treated with pooled sucrose gradient fractions for 24 h and the supernatants were assessed for IL-8 production. No IL-8 was produced by vector-transfected control cells (data not shown). Consistent with the biochemical analysis and distribution of TLR2 agonists in EVs (Fig. 6A), IL-8 production by HEK/hTLR2-CD14 cells was induced

by fractions #8-10 which contain BMVs (Fig. 6B). In contrast, fractions #2-4 (control) and #5-7 (exosomes) did not induce significant levels of IL-8 (Fig. 6B). Thus, exosomes released by Mtb-infected cells did not activate TLR2. To determine the effect of the vesicle subsets on uninfected macrophages, we measured the production of TNF-α, which has been shown in several studies to be induced by EVs from Mtb-infected cells (11, 12, 19). Treatment of murine macrophages for 24 h with the BMV fractions (#8-10), but not the exosome (#5-7) or control (#2-4) fractions led to the release of TNFα. Similar results were observed for IL-12 p40 and IL-10 induction (data not shown). We conclude that the TLR2 agonist and proinflammatory activities attributed to EVs released from Mtb-infected cells derive from Mtb BMVs and not from host cell-derived exosomes.

Discussion

EVs released by Mtb-infected macrophages activate innate and adaptive immune responses to Mtb, but the mechanism for the trafficking of Mtb PAMPs and antigens into EVs has not been elucidated. The existing hypothesis has been that Mtb molecules are released in exosomes (11-15, 17-20) (Fig. 7A). This implies that membrane-associated lipoglycans and lipoproteins are secreted by Mtb in the phagosome, associate with host membranes, and traffic to MVEs where they are incorporated into intraluminal vesicles and released as exosomes upon MVE fusion with the plasma membrane (Fig. 7A). Furthermore, no mechanism has been proposed for the trafficking of soluble Mtb proteins, such as immunodominant antigens, into exosomes (13). This would require that Mtb proteins are translocated to the cytosol and then sorted into intraluminal vesicles of MVEs. Our revised model provides a rationale for Mtb lipoglycan and lipoprotein secretion during infection as well as the trafficking of membrane-associated and soluble Mtb molecules into EVs. Our results indicate that most Mtb molecules released from infected macrophages derive from BMVs that are produced by intracellular Mtb within macrophage phagosomes, traffic through vesicular compartments and are subsequently released by exocytosis into the extracellular environment (Fig. 7B).

Our revised model for the trafficking of Mtb molecules into EVs was first suggested by imaging studies. Immunolabeling and analysis of EVs by electron microscopy and immunofluorescence microscopy identified distinct EV subpopulations that contained host or bacterial molecules (Fig. 2 and 3). To our knowledge, this is the first published study to employ immunofluorescence microscopy for the quantitative analysis of EV composition, and our results indicate that Mtb molecules are largely excluded from host-derived exosomes. This experimental approach has potential broad applicability for the study of EV content and function. The findings from our imaging studies were further corroborated by the separation of EVs containing Mtb molecules from exosomes using sucrose density gradients (Fig. 4 and 6). Taken together, our data demonstrate minimal overlap of host and Mtb markers on EVs released from Mtb-infected cells, leading to the conclusion that these markers are present in two distinct vesicle subpopulations, host-derived exosomes and Mtb-derived BMVs. Our data do not exclude the incorporation of a small proportion of bacterial molecules into host-derived exosomes, but the infrequent occurrence of vesicles that contain both host and bacterial markers (Fig. 2-4) indicates that this is a minor pathway relative to the BMV trafficking pathway.

The bacterial origin of EVs that contain Mtb components is suggested by three findings. First, BMVs produced by Mtb in culture are 40-250 nm in size and enriched for lipoglycans and lipoproteins (23), similar to the EVs that are released by Mtb-infected cells (Fig. 1, 2). Second, the release of EVs containing Mtb components from infected macrophages was dependent on the viability of the Mtb bacterium (Fig. 5A), consistent with studies of BMV production in axenic culture (23). Although one might predict the extensive dissemination of components from dead bacteria, lipoglycans from irradiated or heat-killed Mtb did not traffic into EVs (Fig. 5A). In agreement with our findings, macrophages treated with heat-killed *M. bovis* BCG release EVs, but they are not pro-inflammatory (12). This indicates the absence of cell wall-derived TLR2 agonists such as lipoproteins. Third, electron microscopy analysis of Mtb bacilli isolated from infected macrophages shows the apparent budding of membrane vesicles (Fig. 5B). Taken together, our data support the conclusion that BMV secretion is an active bacterial process that occurs within Mtb-infected cells.

Although we propose a revision to the current paradigm for the trafficking of Mtb molecules into EVs (Fig. 7), we emphasize that prior data are consistent with our results and our revised model (11-15, 17-20). Mtb BMVs produced in axenic culture and EVs produced by Mtb-infected cells induce TLR2-mediated immune regulation (12, 19, 20, 23, 32), much the same as purified Mtb lipoproteins or infection with Mtb (2, 6, 34). Thus, the functional data from prior studies is valid, but we propose a different interpretation regarding the cellular origin of the EVs that traffic Mtb molecules and that regulate host responses to Mtb (11-15, 19, 20). Techniques employed in previous studies for the purification or analysis of EVs produced during Mtb infection could not discriminate between exosomes and Mtb BMVs. For example, the methods used to purify mycobacterial BMVs and mammalian exosomes are often identical, so the use of a final 100,000 × *g* ultracentrifugation step will isolate both types of EVs from a sample (20, 23, 26). Electron microscopy cannot distinguish between exosomes and Mtb BMVs based on size and morphology alone. Furthermore, bulk analyses of EVs released by Mtb-infected cells provide information about the composition and functions of the total EV population, but do not reveal the properties of subpopulations such as BMVs and exosomes. We therefore employed sucrose density gradients to fractionate the EVs released by Mtb-infected cells and determined which vesicle subset mediated biological activities reported in previous studies. Consistent with the enrichment of lipoproteins in the BMV fraction and the absence of Mtb components in the exosome fraction, we only observed TLR2-driven responses and cytokine production when uninfected cells were treated with BMVs (Fig. 6). Taken together, our results indicate the BMVs, not host-derived exosomes, are the EV population responsible for the trafficking of Mtb molecules from infected macrophages *in vitro* and for the regulation of uninfected immune cells. Interestingly, EVs (believed to be exosomes) that contain Mtb antigens have been isolated from the serum of patients with latent and active TB; several of these antigens have also been identified in Mtb BMVs (23, 35). This demonstrates that the release of EVs bearing Mtb components from Mtb-infected cells is physiologically relevant and occurs in the course of human disease. Future studies will address the role of BMVs in the Mtb host-pathogen interaction and the cellular origin of EVs produced during Mtb infection *in vivo*. Furthermore, exosomes released from Mtb-infected cells may have novel immunoregulatory

properties that are mediated by unrelated mechanisms, such as the shuttling of miRNA to uninfected immune cells (16).

Multiple mycobacterial species, including Mtb, produce BMVs in culture and it has been proposed that BMVs serve as a mechanism to secrete membrane-associated Mtb lipoglycans and lipoproteins (23, 32). Our findings agree with this model and provide evidence for the dissemination of Mtb LAM and TLR2 agonists via BMVs within Mtb-infected macrophages. Thus, Mtb BMVs may significantly contribute to Mtb immune evasion mechanisms such as TLR2-dependent modulation of MHC-II antigen presentation and cytokine production in infected cells. The lipoglycan LAM is required for the inhibition of phagosome maturation during Mtb infection (1) and is also present in Mtb BMVs (23). Heat-killed or irradiated Mtb are unable to block phagosome maturation despite containing LAM (25, 36), suggesting a likely and vital role for BMVs in LAM secretion and the inhibition of phagolysosome fusion. Our results also indicate that BMVs produced within Mtb-infected cells are released into the extracellular environment. The extracellular Mtb BMVs may traffic beyond the site of infection and interact with uninfected immune cells, thereby regulating host responses via the delivery of Mtb molecules, such as TLR2 agonists, to uninfected immune cells. Mtb TLR2 agonists have clear regulatory roles for macrophages (3, 5, 24, 37), dendritic cells (38, 39), and T cells (40, 41). Purified LAM has also been shown to directly prevent the activation of CD4+ T cells by interfering with T cell receptor signaling (42, 43). The mechanisms for secretion and trafficking of these molecules by BMVs is an important area for further study.

The study of BMVs is an emerging field and BMVs may play important roles in bacterial pathogenesis. The composition and functions of BMVs vary across species, but BMV production is a conserved mechanism that may be triggered by environmental stress for the purpose of survival (44). Pathogenic bacteria secrete toxins and virulence factors via BMVs, as well as factors that modulate or defend against host immune responses (45). Our studies demonstrate that the release of immunomodulatory Mtb molecules from infected macrophages is driven by BMV secretion, raising many new questions on other potential components and roles of Mtb BMVs in the host-pathogen interaction. The biogenesis of Mtb BMVs and the host factors that induce their release within infected macrophages present two novel areas of research, both of which may lead to a new understanding of Mtb pathogenesis and novel therapeutic strategies for the treatment of TB.

Acknowledgements

We thank Supriya Shukla, Tom Richardson, Roxana Rojas and George Dubyak for helpful advice. Nancy Nagy provided important technical support. Electron microscopy services were provided by Hisashi Fujioka (CWRU Electron Microscopy Core Facility).

Research funding was provided by the following NIH grants: T32 GM008056 (to JJA), R01 AI027243 (to WHB), R01 AI069085 and R01 AI034343 (to CVH), and R21 AI103443 and the Steris Corporation Infectious Disease Award (to PAW). Portions of this research were also made possible with funding (Developmental Award to PAW) and core facility resources of the Case Western Reserve University/University Hospitals Center for AIDS Research, NIH P30 AI036219.

Abbreviations

Mtb	Mycobacterium tuberculosis
LAM	lipoarabinomannan
LM	lipomannan
MHC-II	class II MHC
EV	extracellular vesicle
BMV	bacterial membrane vesicle
MOI	multiplicity of infection
MVE	multivesicular endosome

References

1. Fratti RA, Chua J, Vergne I, Deretic V. Mycobacterium tuberculosis glycosylated phosphatidylinositol causes phagosome maturation arrest. Proc. Natl. Acad. Sci. USA. 2003; 100:5437–5442. [PubMed: 12702770]
2. Harding CV, Boom WH. Regulation of antigen presentation by Mycobacterium tuberculosis: a role for Toll-like receptors. Nature Rev. Microbiol. 2010; 8:296–307. [PubMed: 20234378]
3. Pennini ME, Pai RK, Schultz DC, Boom WH, Harding CV. Mycobacterium tuberculosis 19-kDa lipoprotein inhibits IFN-gamma-induced chromatin remodeling of MHC2TA by TLR2 and MAPK signaling. J. Immunol. 2006; 176:4323–4330. [PubMed: 16547269]
4. Noss EH, Pai RK, Sellati TJ, Radolf JD, Belisle J, Golenbock DT, Boom WH, Harding CV. Toll-like receptor 2-dependent inhibition of macrophage class II MHC expression and antigen processing by 19 kD lipoprotein of Mycobacterium tuberculosis. J. Immunol. 2001; 167:910–918. [PubMed: 11441098]
5. Pai RK, Convery M, Hamilton TA, Boom WH, Harding CV. Inhibition of IFN-gamma-induced class II transactivator expression by a 19-kDa lipoprotein from Mycobacterium tuberculosis: a potential mechanism for immune evasion. J. Immunol. 2003; 171:175–184. [PubMed: 12816996]
6. Kincaid EZ, Wolf AJ, Desvignes L, Mahapatra S, Crick DC, Brennan PJ, Pavelka MS Jr. Ernst JD. Codominance of TLR2-dependent and TLR2-independent modulation of MHC class II in Mycobacterium tuberculosis infection in vivo. J. Immunol. 2007; 179:3187–3195. [PubMed: 17709534]
7. Saraiva M, O'Garra A. The regulation of IL-10 production by immune cells. Nat Rev Immunol. 2010; 10:170–181. [PubMed: 20154735]
8. Richardson ET, Shukla S, Sweet DR, Wearsch PA, Tsichlis PN, Boom WH, CV H. TLR2-dependent ERK signaling in *Mycobacterium tuberculosis*-infected macrophages drives anti-inflammatory responses and inhibits Th1 polarization of responding T cells. Infect Immun. 2015 In press.
9. Beamer GL, Flaherty DK, Assogba BD, Stromberg P, Gonzalez-Juarrero M, de Waal Malefyt R, Vesosky B, Turner J. Interleukin-10 promotes Mycobacterium tuberculosis disease progression in CBA/J mice. J. Immunol. 2008; 181:5545–5550. [PubMed: 18832712]
10. Beatty WL, Rhoades ER, Ullrich HJ, Chatterjee D, Heuser JE, Russell DG. Trafficking and release of mycobacterial lipids from infected macrophages. Traffic. 2000; 1:235–247. [PubMed: 11208107]
11. Bhatnagar S, Schorey JS. Exosomes released from infected macrophages contain Mycobacterium avium glycopeptidolipids and are proinflammatory. J. Biol. Chem. 2007; 282:25779–25789. [PubMed: 17591775]

12. Bhatnagar S, Shinagawa K, Castellino FJ, Schorey JS. Exosomes released from macrophages infected with intracellular pathogens stimulate a proinflammatory response in vitro and in vivo. Blood. 2007; 110:3234–3244. [PubMed: 17666571]
13. Giri PK, Kruh NA, Dobos KM, Schorey JS. Proteomic analysis identifies highly antigenic proteins in exosomes from M. tuberculosis-infected and culture filtrate protein-treated macrophages. Proteomics. 2010
14. Beatty WL, Ullrich HJ, Russell DG. Mycobacterial surface moieties are released from infected macrophages by a constitutive exocytic event. Eur J Cell Biol. 2001; 80:31–40. [PubMed: 11211933]
15. Russell DG. Who puts the tubercle in tuberculosis? Nat Rev Microbiol. 2007; 5:39–47. [PubMed: 17160001]
16. Raposo G, Stoorvogel W. Extracellular vesicles: exosomes, microvesicles, and friends. J Cell Biol. 2013; 200:373–383. [PubMed: 23420871]
17. Ramachandra L, Qu Y, Wang Y, Lewis CJ, Cobb B, Takatsu K, Boom WH, Dubyak GR, Harding CV. Mycobacterium tuberculosis synergizes with ATP to induce release of microvesicles and exosomes containing major histocompatibility complex class II molecules capable of antigen presentation. Infect. Immun. 2010; 78:5116–5125. [PubMed: 20837713]
18. Giri PK, Schorey JS. Exosomes derived from M. Bovis BCG infected macrophages activate antigen-specific CD4+ and CD8+ T cells in vitro and in vivo. PLoS ONE. 2008; 3:e2461. [PubMed: 18560543]
19. Singh PP, Smith VL, Karakousis PC, Schorey JS. Exosomes isolated from mycobacteria-infected mice or cultured macrophages can recruit and activate immune cells in vitro and in vivo. J Immunol. 2012; 189:777–785. [PubMed: 22723519]
20. Singh PP, LeMaire C, Tan JC, Zeng E, Schorey JS. Exosomes released from M. tuberculosis infected cells can suppress IFN-gamma mediated activation of naive macrophages. PLoS One. 2011; 6:e18564. [PubMed: 21533172]
21. Thery C, Ostrowski M, Segura E. Membrane vesicles as conveyors of immune responses. Nat Rev Immunol. 2009; 9:581–593. [PubMed: 19498381]
22. Harding C, Heuser J, Stahl P. Receptor-mediated endocytosis of transferrin and recycling of the transferrin receptor in rat reticulocytes. J. Cell Biol. 1983; 97:329–339. [PubMed: 6309857]
23. Prados-Rosales R, Baena A, Martinez LR, Luque-Garcia J, Kalscheuer R, Veeraraghavan U, Camara C, Nosanchuk JD, Besra GS, Chen B, Jimenez J, Glatman-Freedman A, Jacobs WR Jr. Porcelli SA, Casadevall A. Mycobacteria release active membrane vesicles that modulate immune responses in a TLR2-dependent manner in mice. J Clin Invest. 2011; 121:1471–1483. [PubMed: 21364279]
24. Pecora ND, Gehring AJ, Canaday DH, Boom WH, Harding CV. Mycobacterium tuberculosis LprA is a lipoprotein agonist of TLR2 that regulates innate immunity and APC function. J. Immunol. 2006; 177:422–429. [PubMed: 16785538]
25. Ramachandra L, Smialek JL, Shank SS, Convery M, Boom WH, Harding CV. Phagosomal processing of Mycobacterium tuberculosis antigen 85B is modulated independently of mycobacterial viability and phagosome maturation. Infect Immun. 2005; 73:1097–1105. [PubMed: 15664953]
26. Thery C, Amigorena S, Raposo G, Clayton A. Isolation and characterization of exosomes from cell culture supernatants and biological fluids. Curr Protoc Cell Biol. 2006 Chapter 3: Unit 3 22.
27. Qu Y, Ramachandra L, Mohr S, Franchi L, Harding CV, Nunez G, Dubyak GR. P2X7 receptor-stimulated secretion of MHC class II-containing exosomes requires the ASC/NLRP3 inflammasome but is independent of caspase-1. J. Immunol. 2009; 182:5052–5062. [PubMed: 19342685]
28. Li J, Liu K, Liu Y, Xu Y, Zhang F, Yang H, Liu J, Pan T, Chen J, Wu M, Zhou X, Yuan Z. Exosomes mediate the cell-to-cell transmission of IFN-alpha-induced antiviral activity. Nat Immunol. 2013; 14:793–803. [PubMed: 23832071]
29. Deatherage BL, Cookson BT. Membrane vesicle release in bacteria, eukaryotes, and archaea: a conserved yet underappreciated aspect of microbial life. Infect Immun. 2012; 80:1948–1957. [PubMed: 22409932]

30. Kulp A, Kuehn MJ. Biological functions and biogenesis of secreted bacterial outer membrane vesicles. Annu Rev Microbiol. 2010; 64:163–184. [PubMed: 20825345]
31. Berleman J, Auer M. The role of bacterial outer membrane vesicles for intra- and interspecies delivery. Environ Microbiol. 2013; 15:347–354. [PubMed: 23227894]
32. Rath P, Huang C, Wang T, Wang T, Li H, Prados-Rosales R, Elemento O, Casadevall A, Nathan CF. Genetic regulation of vesiculogenesis and immunomodulation in Mycobacterium tuberculosis. Proc Natl Acad Sci U S A. 2013; 110:E4790–4797. [PubMed: 24248369]
33. Prados-Rosales R, Weinrick BC, Pique DG, Jacobs WR Jr. Casadevall A, Rodriguez GM. A role for Mycobacterium tuberculosis membrane vesicles in iron acquisition. J Bacteriol. 2014; 196:1250–1256. [PubMed: 24415729]
34. Pai RK, Pennini ME, Tobian AA, Canaday DH, Boom WH, Harding CV. Prolonged toll-like receptor signaling by Mycobacterium tuberculosis and its 19-kilodalton lipoprotein inhibits gamma interferon-induced regulation of selected genes in macrophages. Infect. Immun. 2004; 72:6603–6614. [PubMed: 15501793]
35. Kruh-Garcia NA, Wolfe LM, Chaisson LH, Worodria WO, Nahid P, Schorey JS, Davis JL, Dobos KM. Detection of Mycobacterium tuberculosis peptides in the exosomes of patients with active and latent M. tuberculosis infection using MRM-MS. PLoS One. 2014; 9:e103811. [PubMed: 25080351]
36. Ramachandra L, Noss E, Boom WH, Harding CV. Processing of Mycobacterium tuberculosis antigen 85B involves intraphagosomal formation of peptide-major histocompatibility complex II complexes and is inhibited by live bacilli that decrease phagosome maturation. J. Exp. Med. 2001; 194:1421–1432. [PubMed: 11714749]
37. Drage MG, Tsai HC, Pecora ND, Cheng TY, Arida AR, Shukla S, Rojas RE, Seshadri C, Moody DB, Boom WH, Sacchettini JC, Harding CV. Mycobacterium tuberculosis lipoprotein LprG (Rv1411c) binds triacylated glycolipid agonists of Toll-like receptor 2. Nature Struct. Mol. Biol. 2010; 17:1088–1095. [PubMed: 20694006]
38. Simmons DP, Canaday DH, Liu Y, Li Q, Huang A, Boom WH, Harding CV. Mycobacterium tuberculosis and TLR2 agonists inhibit induction of type I IFN and class I MHC antigen cross processing by TLR9. J. Immunol. 2010; 185:2405–2415. [PubMed: 20660347]
39. Drage MG, Pecora ND, Hise AG, Febbraio M, Silverstein RL, Golenbock DT, Boom WH, Harding CV. TLR2 and its co-receptors determine responses of macrophages and dendritic cells to lipoproteins of Mycobacterium tuberculosis. Cell. Immunol. 2009; 258:29–37. [PubMed: 19362712]
40. Reba SM, Li Q, Onwuzulike S, Ding X, Karim AF, Hernandez Y, Fulton SA, Harding CV, Lancioni CL, Nagy N, Rodriguez ME, Wearsch PA, Rojas RE. TLR2 engagement on CD4 T cells enhances effector functions and protective responses to Mycobacterium tuberculosis. Eur. J. Immunol. 2014; 44:1410–1421. [PubMed: 24497180]
41. Lancioni CL, Li Q, Thomas JJ, Ding X, Thiel B, Drage MG, Pecora ND, Ziady AG, Shank S, Harding CV, Boom WH, Rojas RE. Mycobacterium tuberculosis lipoproteins directly regulate human memory CD4(+) T cell activation via Toll-like receptors 1 and 2. Infect Immun. 2011; 79:663–673. [PubMed: 21078852]
42. Mahon RN, Sande OJ, Rojas RE, Levine AD, Harding CV, Boom WH. Mycobacterium tuberculosis ManLAM inhibits T-cell-receptor signaling by interference with ZAP-70, Lck and LAT phosphorylation. Cell Immunol. 2012; 275:98–105. [PubMed: 22507872]
43. Mahon RN, Rojas RE, Fulton SA, Franko JL, Harding CV, Boom WH. Mycobacterium tuberculosis cell wall glycolipids directly inhibit CD4+ T-cell activation by interfering with proximal T-cell-receptor signaling. Infect Immun. 2009; 77:4574–4583. [PubMed: 19651854]
44. Manning AJ, Kuehn MJ. Functional advantages conferred by extracellular prokaryotic membrane vesicles. J Mol Microbiol Biotechnol. 2013; 23:131–141. [PubMed: 23615201]
45. MacDonald IA, Kuehn MJ. Offense and defense: microbial membrane vesicles play both ways. Res Microbiol. 2012; 163:607–618. [PubMed: 23123555]

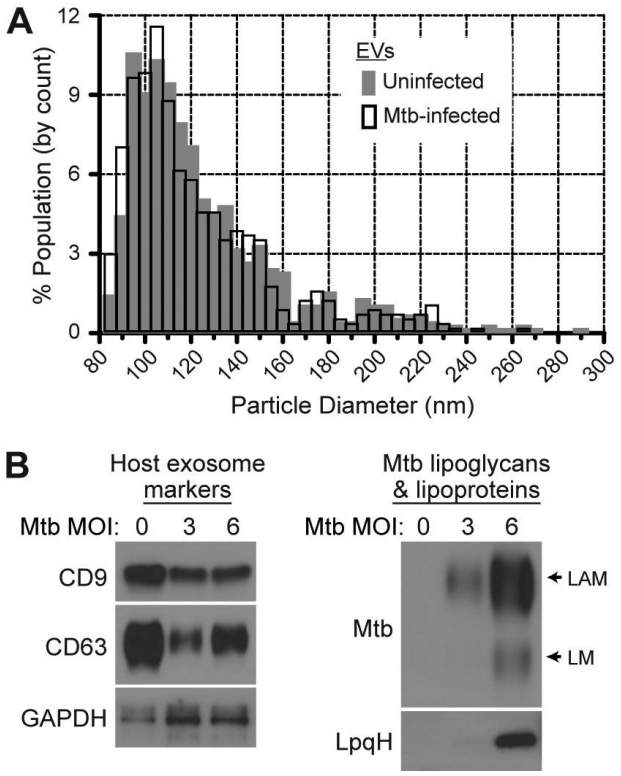

Figure 1.

Mtb-infected macrophages release EVs that contain host exosome markers and Mtb molecules. Macrophages were infected with Mtb for 4 h, washed, and incubated for 20 h in vesicle production medium. EVs were purified from the conditioned culture medium by differential ultracentrifugation and analyzed for composition and size. (**A**) Size distribution of EVs released by uninfected and Mtb-infected (MOI =5) macrophages. Purified EVs were analyzed by tunable resistive pulse sensing using the Izon qNano system. (**B**) EVs released by uninfected (MOI = 0) and Mtb-infected macrophages (MOI = 3 or 6) were analyzed by Western blotting for exosome markers (CD9, CD63, and GAPDH) or Mtb molecules. The polyclonal anti-Mtb Ab primarily detects the lipoglycans LAM and LM. Results are representative of at least three independent experiments.

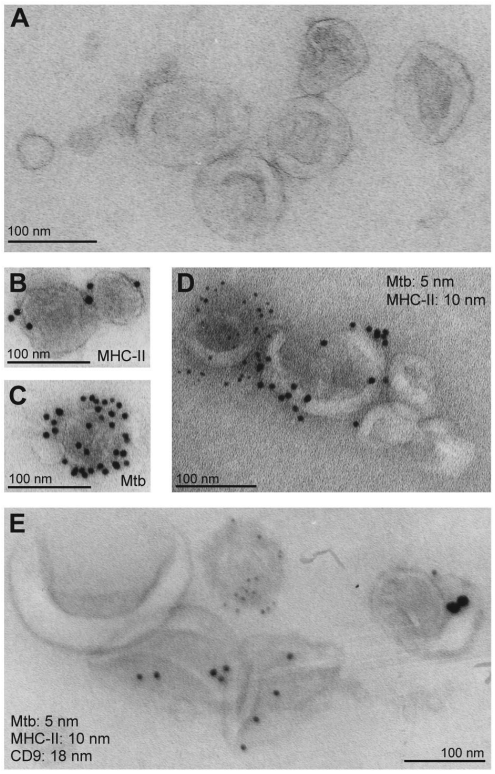

Figure 2.

Immunoelectron microscopy of EVs released by Mtb-infected macrophages reveals distinct subpopulations of vesicles bearing Mtb or exosome markers. EVs were purified from the culture supernatants of Mtb-infected macrophages, fixed, and analyzed by whole mount electron microscopy. (**A**) EVs appear as vesicles with a cup-like morphology. (**B**) Single immunogold labeling of EVs for MHC-II, a component of exosomes released by macrophages. (**C**), Single immunogold labeling of EVs using the anti-Mtb Ab. (**D**) Dual immunogold labeling of EVs with antibodies against MHC-II (10 nm gold particles) and Mtb (5 nm gold particles). (**E**) Triple immunogold labeling of EVs with antibodies against Mtb, MHC-II, and CD9 (5, 10 and 18 nm gold particles, respectively). All scale bars are 100 nm.

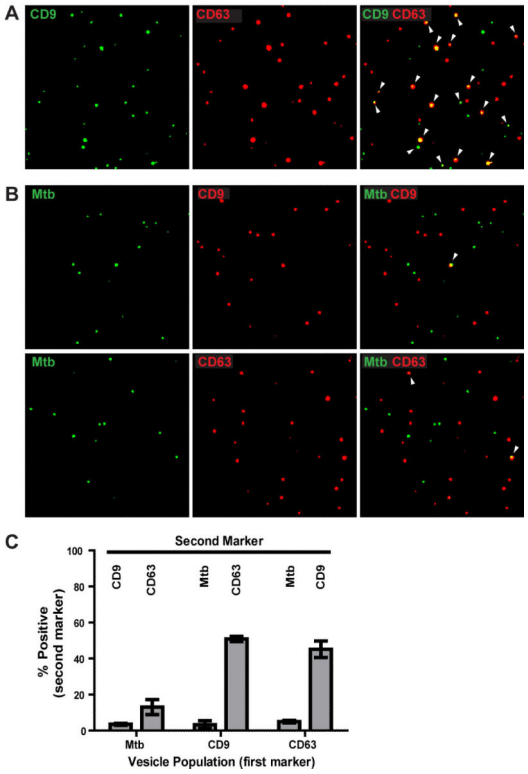

Figure 3.

Immunofluorescence microscopy reveals that EVs from Mtb-infected macrophages are comprised of subpopulations with largely non-overlapping distributions of host and bacterial markers. Purified EVs from Mtb-infected macrophages were fixed on coverslips, stained for host and Mtb markers, and visualized by immunofluorescence microscopy. Each dot represents an individual vesicle. Colocalization of two markers within a vesicle is indicated by white arrowheads (right panels). (**A**) Immunofluorescence staining for two host markers (CD9, green; CD63, red). Images reveal significant overlap between the two host markers. (**B**) Immunofluorescence staining for Mtb (green) and a host marker (CD63 or CD9, red). Images reveal little overlap between host and Mtb markers. Images are representative of more than three independent experiments. (**C**) Colocalization analysis from two independent experiments (values represent mean ± SD.) The quantitation is expressed as the percentage of each vesicle population (Mtb+, CD63+, or CD9+ EVs; x-axis labels) that is positive for a second marker (indicated by labels at the top of the graph).

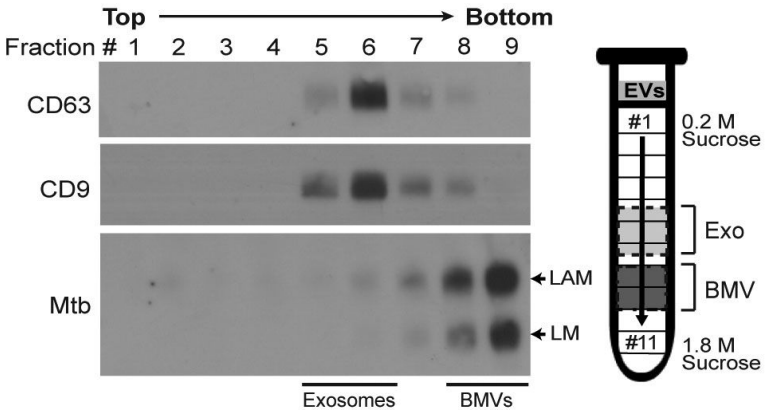

Figure 4.

EVs subpopulations bearing exosome and Mtb molecules can be separated by sucrose density gradient centrifugation. Macrophages were infected for 4 h with Mtb (MOI = 5), washed and incubated for 20 h. EVs were purified by differential ultracentrifugation from the conditioned medium, overlaid on a continuous 0.2-1.8 M sucrose gradient, and centrifuged for 19 h at 110,000 × *g*. Gradient fractions were collected and analyzed by Western blotting with Abs specific for exosome or Mtb molecules. Results are representative of three independent experiments.

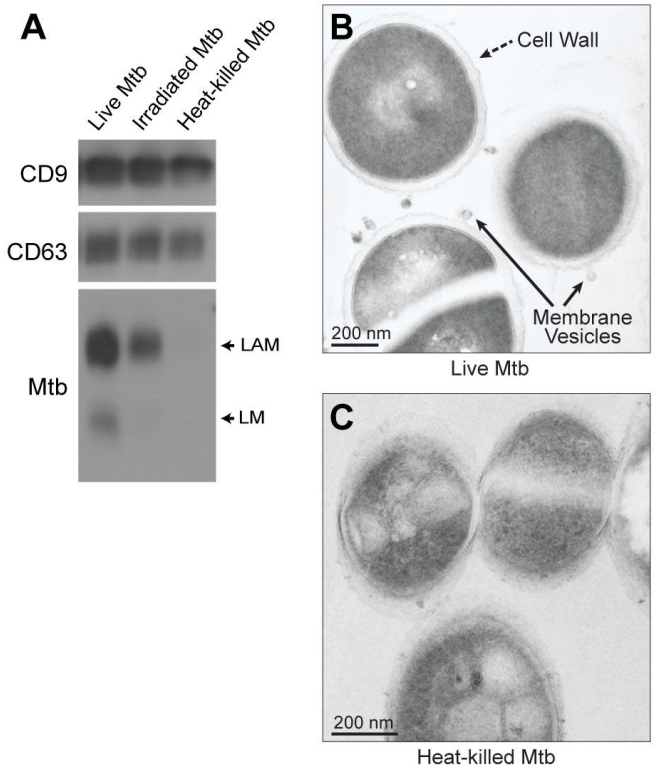

Figure 5.

Release of BMVs from intracellular Mtb is dependent on bacterial viability. (**A**) Macrophages were incubated for 4 h at an MOI or MOI equivalent of 5 with live Mtb, irradiated Mtb (60,000 rad with a ^{137}Cs source; viability reduced by 99.87%), or heat-killed Mtb (80° C for 30 min; viability reduced by 100%). Macrophages were washed and incubated for 20 h. EVs were purified from the conditioned medium and assessed for host or Mtb markers. Results are representative of three independent experiments. (**B, C**) RAW264.7 macrophages were infected for 2 h at an MOI or MOI equivalent of 20 with live Mtb (**B**) or heat-killed Mtb (**C**), washed to remove extracellular bacteria, and then disrupted by Dounce homogenization to release intracellular bacteria. Bacteria were isolated from macrophage homogenates on Percoll gradients and then analyzed by transmission electron microscopy.

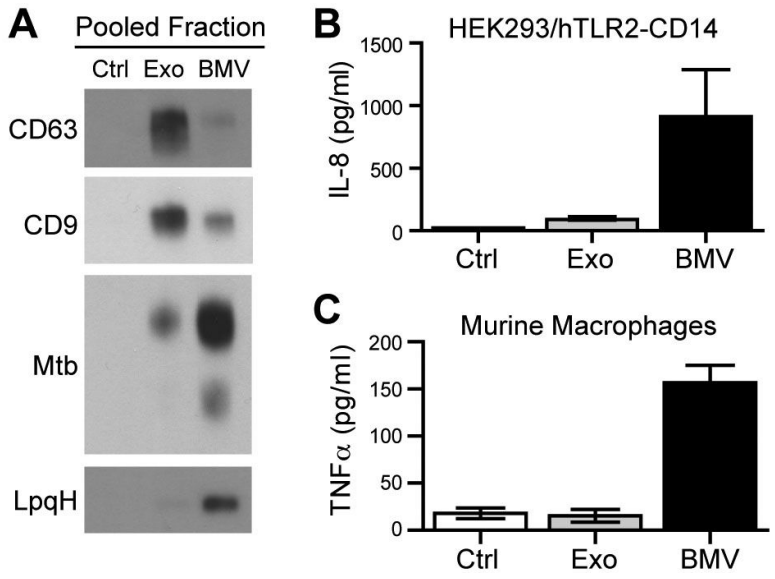

Figure 6.

TLR2 signaling and cytokine production are induced by BMVs but not exosomes from Mtb-infected macrophages. (**A**) EVs released from Mtb-infected cells were purified by differential centrifugation and separated on sucrose density gradients. Fractions were pooled (#2-4, no vesicle control; #5-7, exosomes; #8-10 BMVs), concentrated, exchanged into DMEM culture medium, and analyzed for host and bacterial markers by Western blotting. Results are representative of two independent experiments. (**B**) HEK cells transfected with human TLR2 and CD14 were treated with the indicated sucrose gradient fractions for 24 h. TLR2 activation was assessed by ELISA for the production of IL-8. Results are the average of two replicates and are representative of two independent experiments. (**C**) Murine macrophages were incubated with the pooled sucrose gradient fractions for 24 h and TNF-α production was assessed by ELISA. Results are the average of two replicates and are representative of three independent experiments.

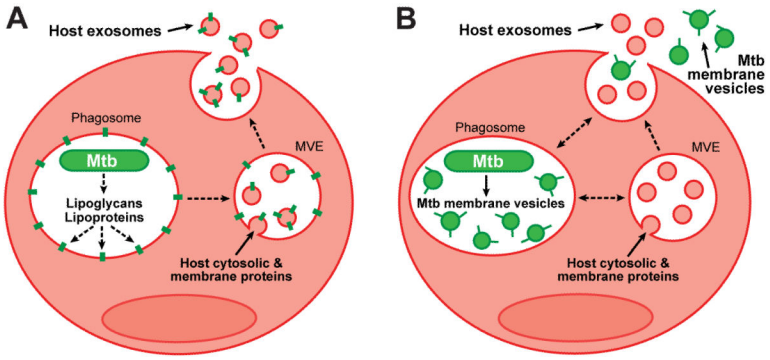

Figure 7.

Proposed models for the trafficking of Mtb molecules into EVs and their release from Mtb-infected macrophages. (**A**) Existing model: extracellular release of Mtb molecules within exosomes. This model predicts that Mtb cell wall components are released from Mtb within the phagosome, inserted into host membranes, and transported to MVEs, where they are incorporated into inclusion vesicles (alternatively inclusion vesicles could be formed by analogous mechanisms within phagosomes). Exosomes bearing Mtb molecules are then released by exocytosis upon MVE fusion with the plasma membrane. (**B**) Revised model: extracellular release of Mtb molecules within BMVs. This model predicts that Mtb employs the release of BMVs as a mechanism to export Mtb molecules such as lipoglycans and lipoproteins. BMVs are produced by intracellular Mtb within the phagosome, dispersed through the endocytic system of the infected cell, and exocytosed in a manner similar to exosomes.